Analysis of Certain Transmission-Line Networks in the Time Domain*

W. J. GETSINGER†

Summary—**Many linear components in nondispersive transmission line are made up solely of commensurate lengths of line of various characteristic impedances. Such components have impulse responses that are a series of equispaced impulses, and, as a result, their frequency responses can be written as a Fourier series. Given the period and coefficients of the Fourier series describing the frequency response, the time response of the circuit to any pulse can be written down immediately as a sum of replicas of the applied pulse, each replica having an amplitude given by the coefficient of a term in the series, and occurring at a time determined by the period of that term of the series.**

The pulse responses of stepped transmission-line transformers, backward-coupling hybrids, and branch-line hybrids are determined and, after assuming a simple applied-pulse shape, are plotted.

Introduction

THE use of millimicrosecond pulses requires component bandwidths that can be achieved only in the microwave frequency range. Since the usual problem is to keep pulse distortion as small as possible, nondispersive transmission lines, such as coaxial and strip transmission lines, have an advantage over dispersive lines, such as waveguide.

Many useful TEM transmission-line components contain no frequency-sensitive elements other than lengths of line. When a network has these properties, its responses to an applied pulse of any shape can be determined by making an arithmetic summation of replicas of the applied pulse, each differing from the next only in amplitude and displacement in time. This process avoids the difficulty of integrating with each applied-pulse shape separately to determine the response.

Method of Analysis

Given a network of steady-state frequency response $f(\omega)$, and an input pulse, expressed in time as $g(t)$, it is desired to find the output pulse $G(t)$ from the network.[1–4] If the network is made up entirely of commensurate lengths of nondispersive transmission lines, its frequency response $f(\omega)$ can be expanded (by methods to be described later) as an infinite series of the form

$$f(\omega) = \sum_{n=0}^{\infty} b_n e^{-in\omega T} \tag{1}$$

where b_d is a coefficient specifying magnitude, ω is radian frequency, and T is a specific time interval depending on the particular microwave component being analyzed. The Fourier integral,

$$f(t) = \int_{-\infty}^{\infty} f(\omega) e^{i\omega t} d\omega, \tag{2}$$

where t is time, can be used to transform $f(\omega)$ into the time domain. When (2) is applied to (1), the result is

$$f(t) = \sum_{n=0}^{\infty} b_n \delta(t - nT) \tag{3}$$

where $\delta(t-nT)$ is a unit impulse occurring at time $t=nT$. This is the network impulse response, and is seen to consist of a series of impulses. The response $G(t)$ of the network to an applied pulse $g(t)$ is found by convolving $f(t)$ and $g(t)$. Convolution is described by

$$G(t) = \int_0^t g(\theta) f(t - \theta) d\theta = g(t) * f(t) \tag{4}$$

where $G(t)$ is the network response, and θ is merely a variable of integration. The lower limit is zero because the input pulse $g(t)$ is assumed to be zero before $t=0$.

Substituting (3) into (4) gives the response of the network to $g(t)$ as

$$G(t) = b_0 g(t) + b_1 g(t - T) + b_2 g(t - 2T) + \cdots \tag{5}$$

because convolution with an impulse yields a replica of the given function.

Comparison of (5) with (1) shows that if the factor T and the coefficients b_k of the frequency response of the network are known, then the response of the network to any pulse can be written down immediately as a series of replicas of the applied pulse.

The frequency response of a network is usually given in closed form, and it is necessary to expand it in order to find the pulse response. The frequency response (1) is periodic with a period $2\pi/T$, and its real part is an even function; thus, the real part of the given frequency response can be expanded in a Fourier series as

$$\mathrm{Re}\, f(\omega) = b_0 + b_1 \cos \omega T + b_2 \cos 2\omega T + \cdots \tag{6}$$

by well-known analytical or numerical methods. The coefficients b_k in (6) may be identified with those in (5), so that the pulse response of the network is known upon

* Manuscript received by the PGMTT, October 9, 1959; revised manuscript received, November 30, 1959. This work was supported by the International Business Machines Corp., Yorktown Heights, N. Y.

† Stanford Res. Inst., Menlo Park, Calif.

[1] S. Goldman, "Frequency Analysis, Modulation, and Noise," McGraw-Hill Book Co., Inc., New York, N. Y., 1st ed., pp. 125–129; 1948.

[2] M. E. Van Valkenburg, "Network Analysis," Prentice-Hall Inc., Englewood Cliffs, N. J., pp. 165, 166; 1955.

[3] E. A. Guillemin, "Communication Networks," John Wiley and Sons, Inc., New York, N. Y., vol. 2, ch. 11, pp. 461–507; 1935.

[4] E. A. Guillemin, "The Fourier integral—a basic introduction," IRE TRANS. ON CIRCUIT THEORY, vol. CT-2, pp. 227–230; September, 1955.

expanding only the real part of its frequency response. Real-part sufficiency is discussed extensively by Guillemin.[5]

Another method of determining the coefficients to be used in (5) is by replacing each $e^{-j\omega T}$ by ζ in the given frequency response, and expanding the function in a power series in ζ about $\zeta=0$, using any of the available methods for determining power series coefficients. The coefficients of the power series are the same as those of the Fourier series for the same values of n, as can be determined by replacing each ζ in the series with $e^{-j\omega T}$ when the expansion has been made. The substitution is possible because the networks being considered involve only commensurate lengths of nondispersive transmission line as frequency-sensitive elements, and thus the independent variable can be considered to be $(e^{-j\omega T})$ rather than ω.

Pulse Response of Stepped Transformers

A properly designed, stepped, transmission-line transformer[6] provides a means of joining two transmission lines of greatly different characteristic impedances without incurring a large mismatch. A diagram of the general step transformer to be discussed is given in Fig. 1. Assumptions made are that the transmission line is nondispersive, that junction effects can be ignored, that the physical distance between adjacent steps is the same for all steps, and that the electrical distance between adjacent steps is one-quarter wavelength at the carrier frequency of the applied pulse.

Determination of Reflected Response

The time-domain reflected-response characteristic of the step transformer will be determined by applying a unit impulse at Step 1 and obtaining the impulse response directly. Practical step transformers are usually well matched, and the reflections from the individual steps are relatively small, so that for the reflected response, signal level can be considered to be the same at each step, and multiple reflections can be ignored. Suppose a unit impulse reaches the first step at $t=0$. There is an immediate reflection at that step. If the time required for the impulse to advance from one step to the next is called T, the reflection from the kth step reaches the first step when $t=2kT$. The amplitude of each response is the voltage reflection factor ρ_k of that particular step. Thus, the reflected impulse response from all n steps can be written as

$$f_r(t) = \sum_{k=1}^{n} \rho_k \delta[t - 2(k-1)T]. \tag{7}$$

From the preceding section, the reflected response to any applied pulse can be written immediately as

$$G_r(t) = \sum_{k=1}^{n} \rho_k g[t - 2(k-1)T]. \tag{8}$$

Let

$$g(t) = e(t) \sin \omega_0 t \tag{9}$$

and

$$\omega_0 T = \pi/2 \tag{10}$$

where $e(t)$ is the time description of the pulse envelope, and ω_0 is the carrier radian frequency. Also,

$$\begin{aligned} \sin\left(\omega_0 t - \frac{\pi}{2}\right) &= -\cos \omega_0 t \\ \sin(\omega_0 t - \pi) &= -\sin \omega_0 t \\ \sin\left(\omega_0 t - \frac{3\pi}{2}\right) &= \cos \omega_0 t \\ \sin(\omega_0 t - 2\pi) &= \sin \omega_0 t. \end{aligned} \tag{11}$$

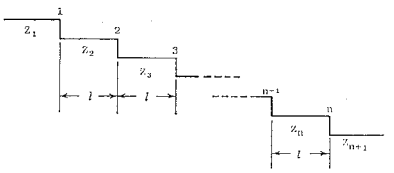

Fig. 1—The stepped transmission-line transformer.

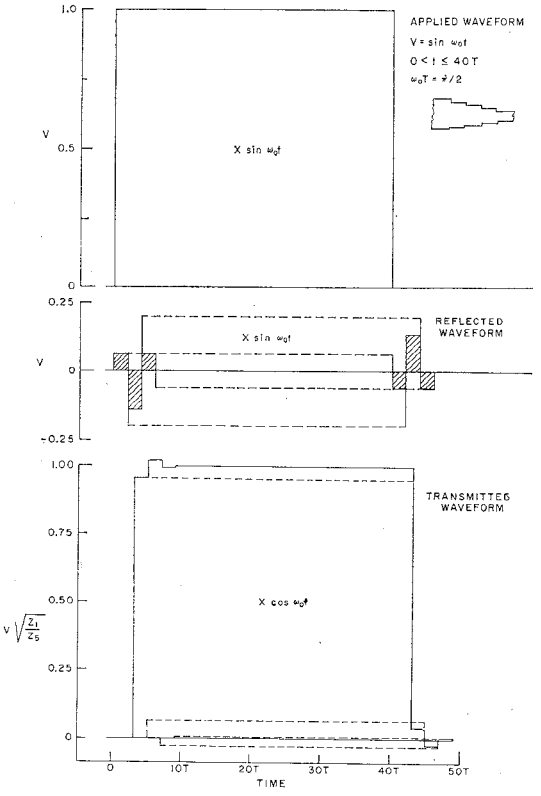

Fig. 2—Response of four-step stepped transmission-line transformer to applied-rectangular pulse.

[5] E. A. Guillemin, "Computational Techniques which Simplify the Correlation Between Steady-State and Transient Response of Filters and Other Networks," *Proc. Natl. Electronics Conf.*, Chicago, Ill., pp. 513–532; 1953.

[6] S. B. Cohn, "Optimum design of stepped transmission-line transformers," IRE Trans. on Microwave Theory and Techniques, vol. MTT-3, pp. 16–21; April, 1955.

Substitution of (9)–(11) into (8) gives

$$G_r(t) = \sin \omega_0 t \left\{ \sum_{k=1}^{n} (-1)^{k+1} \rho_k e[t - 2(k-1)T] \right\}. \quad (12)$$

Expanding for clarity, this becomes

$$G_r(t) = \sin \omega_0 t \{ \rho_1 e(t) - \rho_2 e(t - 2T) + \rho_3 e(t - 4T) - \cdots + \rho_n e[t - 2(n-1)T] \}. \quad (13)$$

The envelope of the pulse reflection response can now be plotted by addition of replicas of the applied envelope reduced in amplitude and displaced in time as given by (12) or (13). This has been done in Fig. 2 for an applied rectangular pulse $40T$ long. The dashed lines indicate the component echoes which add to give the resulting waveshape, indicated by the lined areas, for the reflected wave. Fig. 2 is for a four-step binomial transformer, but the curves do not differ appreciably from those for a four-step Tchebycheff transformer.

Determination of Transmitted Response

The time-domain transmission characteristic of the step transformer has also been determined by following a unit impulse and its significant reflections through the transformer. The unit impulse $\delta(t)$ is applied at Step 1 of Fig. 1. As the impulse travels to the right, it is changed by the voltage transmission coefficient $\vec{\tau}_k$ at each step, and sets up a reflection traveling to the left at each step. Each such reflection is partially reflected again from each step to the left of the step at which it originated. Such re-reflections travel to the right, being changed by $\vec{\tau}_k$ and setting up smaller reflections as each step is passed, and eventually emerge from the right-hand port. The multiple reflections emerging on the right are of the magnitude of $(\rho_k \rho_1)$, $(\rho_k \rho_1)^2$, $(\rho_k \rho_1)^3$, and so on. As $(\rho_k \rho_1)$ is much less than unity for practical transformers, terms of order $(\rho_k \rho_1)^2$ and greater were neglected. Also, products in $\vec{\tau}_i \vec{\tau}_i$ were approximated by unity. Assuming an applied pulse of the form $g(t) = e(t) \sin \omega_0 t$, as was done for the reflected response, the transmitted response $G_t(t)$ can be given in terms of

$$e'(t) = \left(\prod_{1}^{n} \vec{\tau}_k \right) \Bigg\{ e[t - (n-1)T] + \left(\sum_{m=2}^{n} \rho_m \rho_{m-1} \right) e[t - (n+1)T] - \left(\sum_{m=3}^{n} \rho_m \rho_{m-2} \right) e[t - (n+3)T] + \cdots + (-1)^d \left(\sum_{m=d+1}^{n} \rho_m \rho_{m-d} \right) \cdot e[t - (n + 2d - 1)T] + \text{etc.} \Bigg\} \quad (14)$$

where

$e'(t)$ = the output envelope function

$$\begin{aligned} G_t(t) &= (\cos \omega_0 t) e'(t) && \text{for } n = 4, 8, 12, \cdots \\ G_t(t) &= -(\cos \omega_0 t) e'(t) && \text{for } n = 2, 6, 10, \cdots \\ G_t(t) &= (\sin \omega_0 t) e'(t) && \text{for } n = 5, 9, 13, \cdots \\ G_t(t) &= -(\sin \omega_0 t) e'(t) && \text{for } n = 3, 7, 11, \cdots . \end{aligned} \quad (15)$$

Fig. 2 also shows the envelope of the transmitted response of a four-step, binomial, stepped transformer for an applied rectangular pulse. The pulse width chosen, $40T$, is equivalent to ten cycles of the carrier frequency. The response of a stepped transformer designed on other than a binomial basis would still have features similar to those of the response shown. Fig. 3 has been plotted to show the pulse response of a stepped transformer to the pulse envelope $V(t) = \sin^{1/2} (\pi t / 40T)$, for $0 < t \leq 40T$. The transformer used in computing this response was a four-step Tchebycheff design with a 2:1 bandwidth ratio and 3:1 transformation ratio.

Stepped transformers, and other transmission-line components, have discontinuity reactances that are usually considered to be lumped capacitance or inductance, and thus, such a component might not be

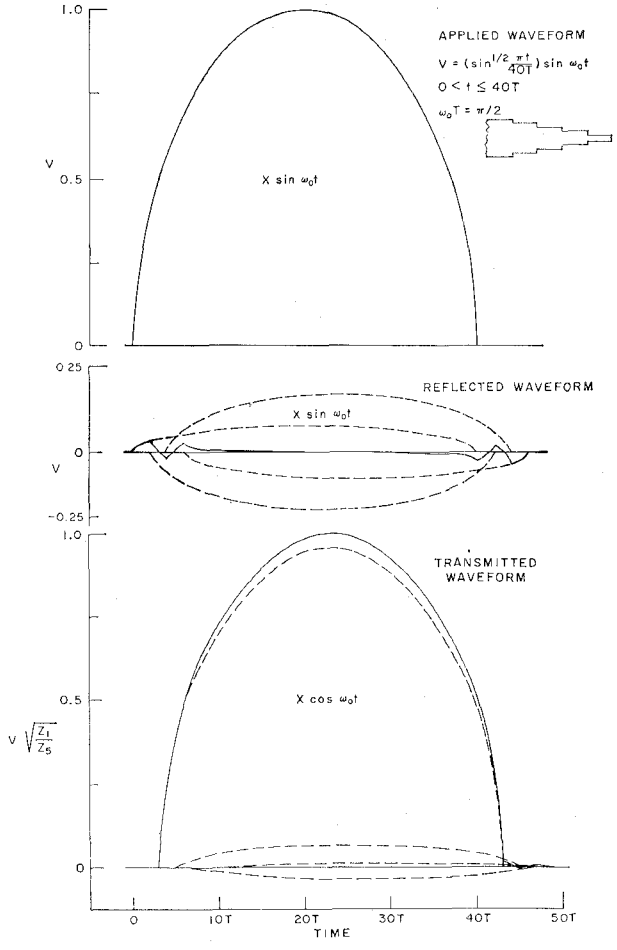

Fig. 3—Response of a four-step stepped transmission-line transformer to applied rounded pulse.

considered suited to pulse analysis by this method. However, it can be shown that reasonably small discontinuity reactances or susceptances, such as are met with in actual components, can be closely approximated by short lengths of nondispersive transmission line, if they are not so small as to be negligible. Thus, discontinuity reactances are not often a serious limitation in pulse analysis by this method.

Pulse Distortion in a Backward-Coupling Hybrid

A backward-coupling hybrid[7–10] is a symmetrical four-port network that divides RF power incident at a given port approximately equally between the port adjacent to and the port collinear with the input port, leaving the diagonally opposite port isolated, as shown in Fig. 4. The impulse responses are given in an article by Oliver,[7] and, thus, the pulse responses can be determined directly. They are:

$$\frac{V_2}{V_1}(t) = \rho g(t) - \rho(1-\rho^2)[g(t-2T) + \rho^2 g(t-4T) + \rho^4 g(t-6T) + \cdots]$$

$$\frac{V_4}{V_1}(t) = (1-\rho^2)[g(t-T) + \rho^2 g(t-3T) + \rho^4 g(t-5T) + \cdots] \quad (16)$$

for an input pulse applied at port 1 of Fig. 4. In these formulas, T is the time required for a unit impulse to traverse the length of the coupler, and ρ is defined by

$$\rho^2 = \frac{1-\sqrt{1-k^2}}{1+\sqrt{1-k^2}}, \quad (17)$$

where k is the midband amplitude coupling factor V_2/V_1. For balanced output, k has the value $\sqrt{2}/2$, and so each term in the brackets of (16) is about 15.35 db down from the preceding term. Thus, only the first few terms have significance in determining pulse distortion.

Pulse Distortion in a Backward-Coupling Hybrid Used as a Sum-and-Difference Network

To consider the backward-coupling hybrid as a sum and difference network, one input port will be Port 1′ of Fig. 4, located a distance $l=\lambda/4$ at the design-center frequency out from Port 1. This has the effect of delaying both output signals from (16) by an additional time T. Now, let identical signals, $g(t)$, be applied at Ports 1′ and 3 at the same instant. By symmetry and superposition, the total signals from Port 2, designated $H_2(t)$, and Port 4, designated $H_4(t)$, are

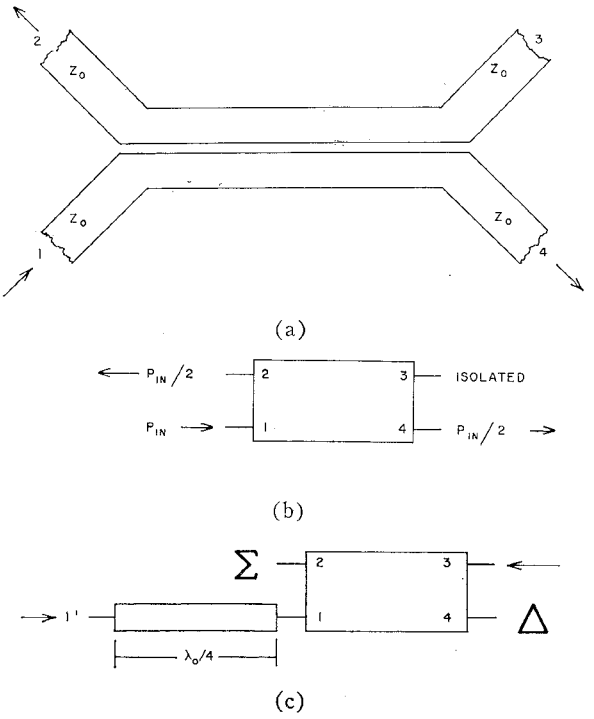

Fig. 4—The backward-coupling hybrid. (a) Physical appearance of conducting center strips. (b) Functional diagram. (c) As a sum-and-difference network.

$$H_2(t) = \frac{V_2}{V_1}(t-T) + \frac{V_4}{V_1}(t)$$

$$H_4(t) = \frac{V_2}{V_1}(t) + \frac{V_4}{V_1}(t-T). \quad (18)$$

Solutions of (18) in terms of the parameters of (16) yield

$$H_2(t) = (1+\rho-\rho^2)g(t-T) - \rho(1-\rho)(1-\rho^2) \cdot [g(t-3T) + \rho^2 g(t-5T) + \rho^4 g(t-7T) + \cdots]$$

$$H_4(t) = \rho g(t) + (1-\rho)(1-\rho^2)[g(t-2T) + \rho^2 g(t-4T) + \rho^4 g(t-6T) + \cdots] \quad (19)$$

where $H_2(t)$ is the Σ output, and $H_4(t)$ the Δ output.

As with the stepped transformers, let $g(t)=e(t)\sin\omega_0 t$, where $e(t)$ is the function describing the envelope of the input pulse, and ω_0, the carrier frequency, is the same as the design-center frequency of the coupler. Using the trigonometric equalities of (15), (19) becomes for the sum arm

$$H_2(t) = -\cos\omega_0 t\{(1+\rho-\rho^2)e(t-T) + \rho(1-\rho)(1-\rho^2)[e(t-3T) - \rho^2 e(t-5T) + \rho^4 e(t-7t) - \cdots]\}, \quad (20)$$

[7] B. M. Oliver, "Directional electromagnetic couplers," Proc. IRE, vol. 42, pp. 1686–1692; November, 1954.
[8] S. B. Cohn, P. M. Sherk, J. K. Shimizu, and E. M. T. Jones, "Strip Transmission Lines and Components," Stanford Res. Inst., Menlo Park, Calif., Final Rept., SRI Project 1114, Contract DA 36-039 SC 63232, DA Project 3-26-00-600,SC Project 2006A; February, 1957.
[9] J. K. Shimizu, "Strip-line 3-db directional couplers," 1957 IRE WESCON Convention Record, pt. 1, pp. 4–9.
[10] J. K. Shimizu and E. M. T. Jones, "Coupled-transmission-line directional couplers," IRE Trans. on Microwave Theory and Techniques, vol. MTT-6, pp. 403–411; October, 1958.

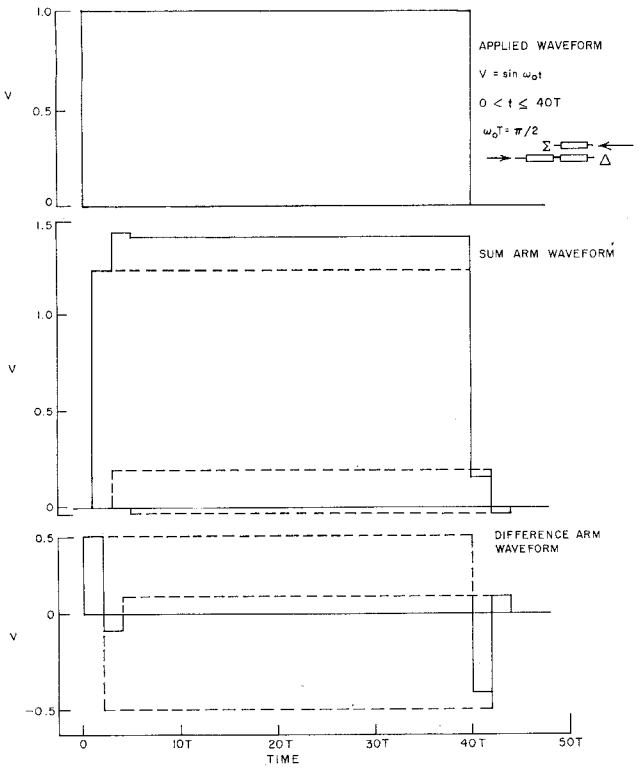

Fig. 5—Responses of backward-coupling hybrid to applied rectangular pulse.

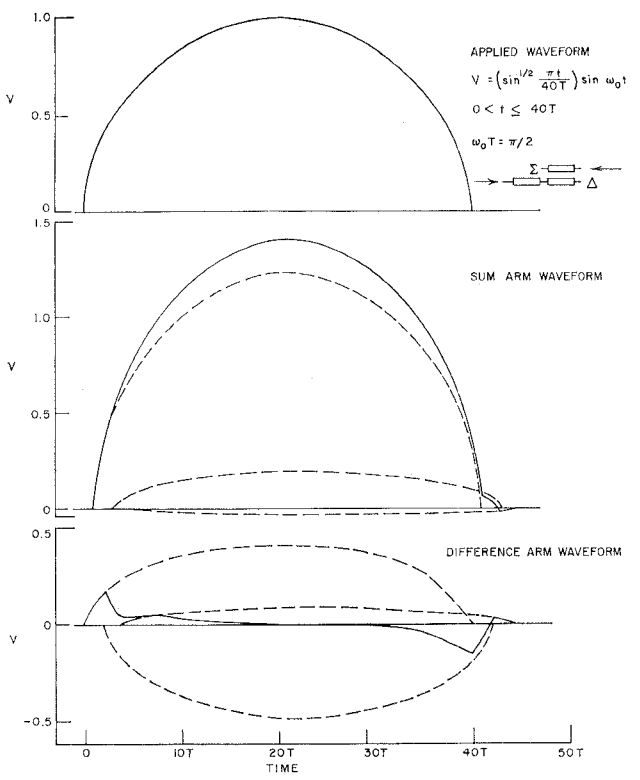

Fig. 6—Responses of backward-coupling hybrid to applied rounded pulse.

for the difference arm

$$H_4(t) = \sin \omega_0 t \{ \rho e(t) - (1-\rho)(1-\rho^2)[e(t-2T) - \rho^2 e(t-4T) + \rho^4 e(t-6T) - \cdots]\}.$$

Substitution of the numerical values $(\sqrt{2}-1)$ for ρ, appropriate for 3-db coupling, gives the pulse shapes for the sum-and-difference arms as

$$H_2(t) = -\cos \omega_0 t \{ 1.24e(t-T) + 0.20e(t-3T) - 0.03e(t-5T)\}$$

for the sum arm, and

$$H_4(t) = \sin \omega_0 t \{ 0.41e(t) - 0.49e(t-2T) + 0.08e(t-4T)\} \quad (21)$$

for the difference arm, where terms of higher order than ρ^2 are omitted, and numbers are rounded off to two places. Any desired accuracy can be obtained by using more terms of the general expression carried out to more decimal places. These equations show that, to the approximation used, all the significant echoes have made their appearance within $4T$ after the appearance of the body of the signal, and have disappeared within $4T$ after the body of the signal has ended.

To illustrate the application of (21), examples of sum-and-difference pulse responses have been plotted in Figs. 5 and 6. The $40T$ pulse width for the envelopes is equivalent to ten cycles of the carrier frequency, denoted ω_0 in (21).

The terms of (21) were added graphically. In general, for a given maximum amplitude of the pulse, the more slowly the pulse rises and falls, the smaller the maximum amplitudes of the distorting terms will be. Thus, a Gaussian-shaped pulse whose maximum slope is less than the maximum slope of the root-sine pulse described above would be expected to have a less-distorted sum-arm output and a smaller-amplitude difference-arm output.

The Branch-Line Coupler as a Sum-and-Difference Network

A coupler well suited to manufacture in strip-line is the branch-line coupler,[11] shown in Fig. 7.

In this section, the frequency response of a certain 3-db branch-line coupler will be given, along with its pulse responses. The pulse responses of the sum-and-difference ports will then be plotted for a number of 3-db branch-line couplers acting as sum-and-difference networks, allowing comparison of different designs on a pulse-response basis.

[11] J. Reed and G. J. Wheeler, "A method of analysis of symmetrical four-port networks," IRE Trans. on Microwave Theory and Techniques, vol. MTT-4, pp. 246–252; October, 1956.

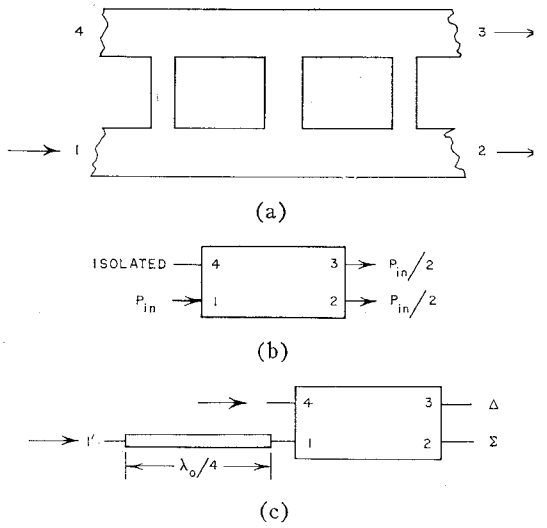

Fig. 7—The branch-line coupler. (a) Physical appearance of conducting center strip. (b) Functional diagram. (c) As a sum-and-difference network.

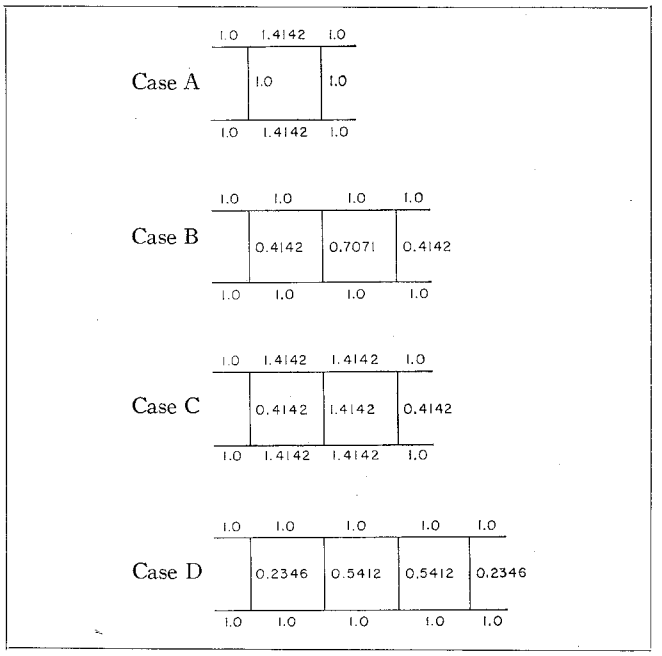

Fig. 8—Relative admittances of arms of 3-db branch-line couplers.

The admittances of the coupler arms relative to the feed-line admittance for the 3-db couplers to be considered in this report are shown in Fig. 8, where each coupler is assigned an identifying letter (A, B, C, and D, in order of increasing bandwidth). These couplers are symmetrical about their centers in all three planes. The electrical distance between adjacent cross-arms is one-quarter wavelength at center frequency, as is the length of each cross-arm. The expressions for the frequency responses of branch-line couplers are quite formidable, and are best handled by an electronic computer, such as the IBM 650.

The pulse responses of these branch-line hybrids were computed by the following method. The frequency responses between the applied signal at Port 1 and scattered signals from each of the four ports were determined by an electronic computer using the procedures of Reed and Wheeler.[11] The real parts of the frequency responses were then taken and their Fourier-series coefficients computed, also by machine. The period of the Fourier series was determined from the physical consideration that the value of the frequency response was the same at $4f_0$ as at zero frequency, where f_0 is the design-center frequency, for all ports of any of the hybrids.

The inverse of the Fourier series period is the time-delay parameter denoted T in the section on Method of Analysis. Thus,

$$T = \frac{1}{4f_0} \cdot \tag{22}$$

This frequency period was used for all the couplers, and in each case it provided the proper time delay between signal application at Port 1 and response at any given port.

It was then necessary only to substitute in (4) to arrive at the time responses of a given coupler to an arbitrary pulse. Assuming a pulse-modulated signal of the form

$$g(t) = e(t) \sin \omega_0 t \tag{9}$$

where $e(t)$ is the envelope description and ω_0 is the design-center radian frequency of the coupler, the responses of Case B are given below for all terms of amplitude greater than 0.001 (relative to the amplitude of the applied pulse), and are plotted in Fig. 9 for a rectangular applied-pulse envelope.

$$\begin{aligned} G_1(t) = \sin \omega_0 t[&-0.172e(t) + 0.366e(t - 2T) \\ &- 0.038e(t - 4T) - 0.111e(t - 6T) \\ &- 0.046e(t - 8T) - 0.009e(t - 10T) \\ &+ 0.004e(t - 12T) + 0.004e(t - 14T) \\ &+ 0.002e(t - 16T)]. \end{aligned}$$

$$\begin{aligned} G_2(t) = -\sin \omega_0 t[&0.507e(t - 2T) + 0.068e(t - 4T) \\ &+ 0.093e(t - 6T) + 0.041e(t - 8T) \\ &+ 0.008e(t - 10T) - 0.004e(t - 12T) \\ &- 0.004e(t - 14T) - 0.002e(t - 16T)]. \end{aligned}$$

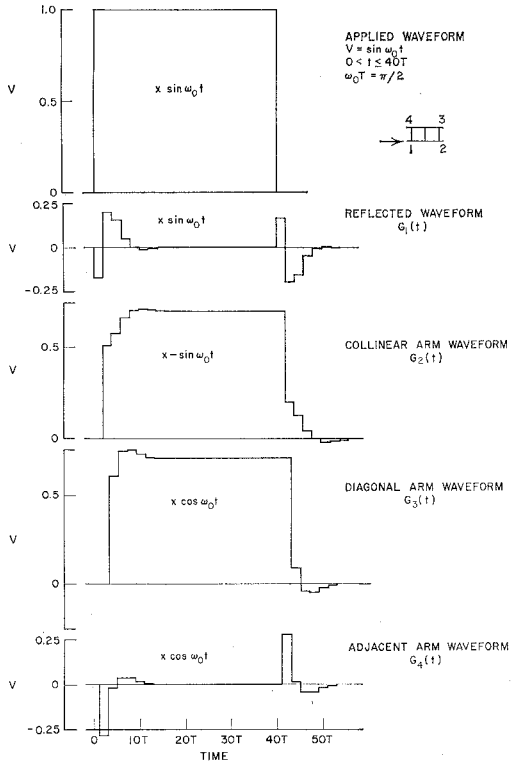

Fig. 9—Responses of 3-db branch-line coupler (Case B) to applied rectangular pulse. (Subscripts refer to port designations applied at Port 1.)

$$
\begin{aligned}
G_3(t) &= \cos\omega_0 t[0.613e(t-3T) + 0.130e(t-5T) \\
&\quad +0.005e(t-7T) - 0.023e(t-9T) \\
&\quad - 0.015e(t-11T) - 0.005e(t-13T)]. \\
G_4(t) &= \cos\omega_0 t[-0.284e(t-T) + 0.265e(t-3T) \\
&\quad + 0.060e(t-5T) - 0.001e(t-7T) \\
&\quad - 0.022e(t-9T) - 0.014e(t-11T) \\
&\quad - 0.005e(t-13T) - 0.000e(t-15T) \\
&\quad + 0.001e(t-17T)].
\end{aligned} \tag{23}
$$

These responses apply only when the applied frequency is exactly the same as the design-center frequency of the coupler. For a small change in applied frequency, the phase of the carrier of each replica is displaced by a small angle from that of the preceding replica, so that the replicas will no longer add exactly in phase. The equations of (23) can be modified to include the effect of such a change in frequency from the design-center frequency, ω_0, to a new frequency, ω_c, by removing the sin $\omega_0 t$ [or cos $\omega_0 t$] preceding the brackets and multiplying each term within the brackets by a factor sin $(\omega_c t - n\phi)$ [or cos $(\omega_c t - n\phi)$] where n is the same integer as in the term $(t - nT)$ giving the envelope displacement for that replica. The value of phase term ϕ is given by

$$\phi = \frac{\pi}{2}\left(\frac{\omega_c}{\omega_0} - 1\right). \tag{24}$$

The addition of a quarter-wavelength of line to one input port makes a sum-and-difference network of the branch-line hybrid. With reference to Fig. 7, assume that identical signals are applied at Ports 1′ and 4 simultaneously. By simple superposition, signal $H_1(t)$, emerging at Port 1′, signal $H_2(t)$, emerging at Port 2, and so on, are given by

$$
\begin{aligned}
H_1(t) &= G_1(t-2T) + G_4(t-T) \\
H_2(t) &= G_2(t-T) + G_3(t) \\
H_3(t) &= G_2(t) + G_3(t-T) \\
H_4(t) &= G_1(t) + G_4(t-T)
\end{aligned} \tag{25}
$$

because the signal takes a time interval T to travel one-quarter wavelength at the center frequency. $H_2(t)$ is the sum response and $H_3(t)$ is the difference response. The following are given for the branch-line hybrid Case B, assuming the signal to be $e(t)$ sin $\omega_0 t$, as before:

$$
\begin{aligned}
H_1(t) &= \sin\omega_0 t[-0.112e(t-2T) - 0.101e(t-4T) \\
&\quad + 0.098e(t-6T) + 0.110e(t-8T) \\
&\quad + 0.024e(t-10T) - 0.005e(t-12T) \\
&\quad - 0.009e(t-14T) - 0.004e(t-16T) \\
&\quad - 0.001e(t-18T)]. \\
H_2(t) &= \cos\omega_0 t[1.120e(t-3T) + 0.199e(t-5T) \\
&\quad + 0.097e(t-7T) + 0.018e(t-9T) \\
&\quad - 0.006e(t-11T) - 0.008e(t-13T) \\
&\quad - 0.004e(t-15T) - 0.002e(t-17T)]. \\
H_3(t) &= \sin\omega_0 t[-0.507e(t-2T) + 0.545e(t-4T) \\
&\quad + 0.038e(t-6T) - 0.036e(t-8T) \\
&\quad - 0.032e(t-10T) - 0.011e(t-12T) \\
&\quad - 0.001e(t-14T) + 0.002e(t-16T)]. \\
H_4(t) &= \sin\omega_0 t[-0.172e(t) + 0.082e(t-2T) \\
&\quad + 0.227e(t-4T) - 0.051e(t-6T) \\
&\quad - 0.047e(t-8T) - 0.031e(t-10T) \\
&\quad - 0.010e(t-12T) - 0.001e(t-14T) \\
&\quad + 0.002e(t-16T)].
\end{aligned} \tag{26}
$$

Figs. 10–13 show the sum-and-difference responses to a rectangular, pulse-modulated signal of the four branch-line couplers (Cases A, B, C, and D). It is interesting that the transients in the response curves for

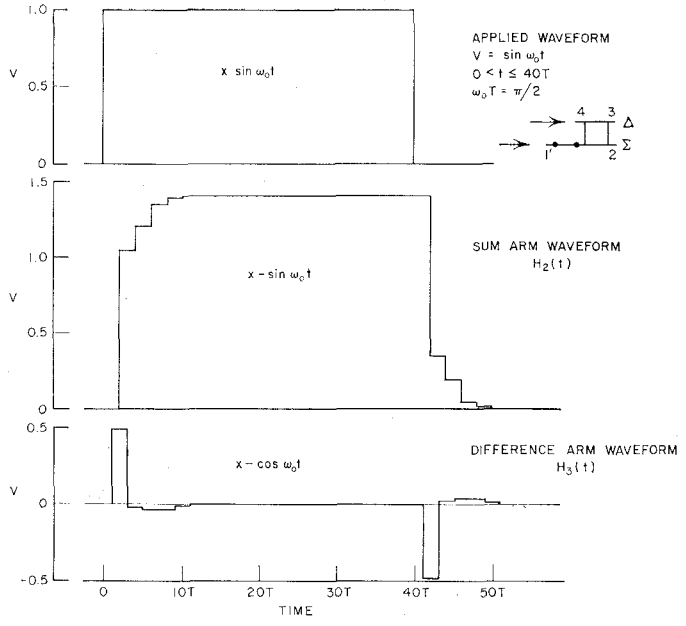

Fig. 10—Sum-and-difference responses of a branch-line coupler (Case A) to applied rectangular pulse.

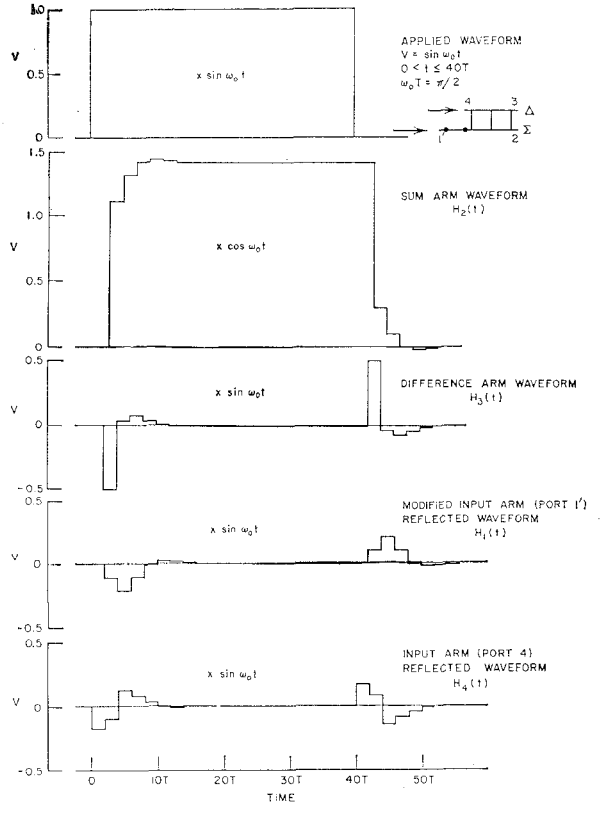

Fig. 11—Sum-and-difference responses of a branch-line coupler (Case B) to applied rectangular pulse.

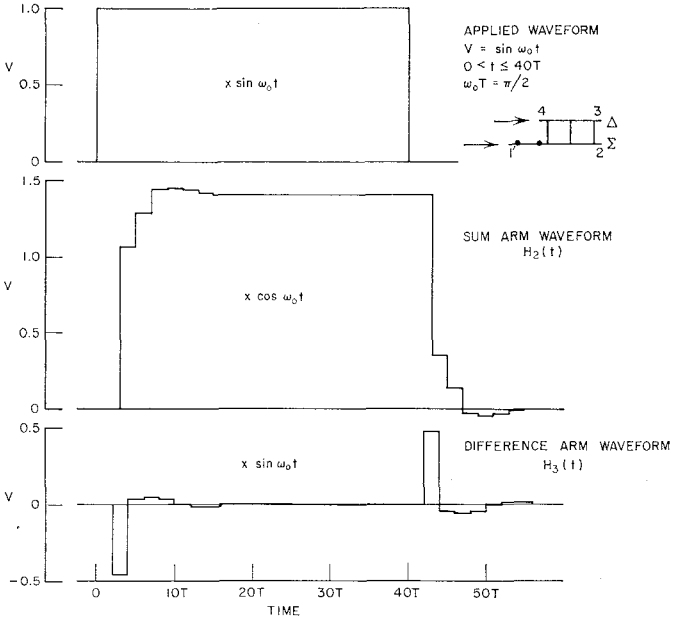

Fig. 12—Sum-and-difference responses of a branch-line coupler (Case C) to applied rectangular pulse.

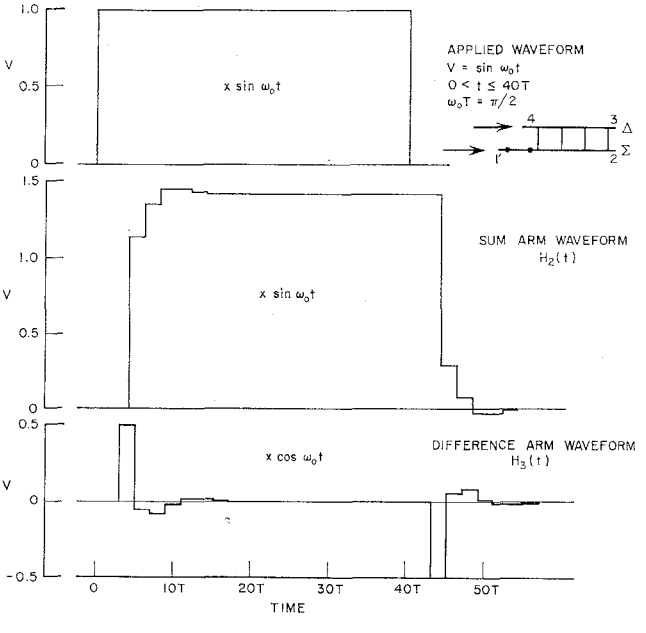

Fig. 13—Sum-and-difference responses of a branch-line coupler (Case D) to applied rectangular pulse.

the branch-line couplers and the sum-and-difference networks are of appreciable magnitude for only three cycles or less of the carrier frequency. Thus, in passing through these components, pulses only three cycles long, or spaced from each other by only three cycles, retain their general shape and identity.

Conclusion

It has been shown that the pulse responses of microwave components, made of nondispersive transmission lines only, are sums of replicas of the applied pulse. Two different ways were described by which the amplitudes and times of occurrence of the individual replicas can be found from the component frequency responses or impulse responses.

This technique for finding pulse responses was applied to stepped transmission-line transformers, to the backward coupler as a hybrid and sum-and-difference networks, and to branch-line couplers as hybrids and sum-and-difference networks. It was found that rectangular-pulse envelopes lasting for only three periods of the carrier frequency would pass through any one of these components without extreme distortion.

Acknowledgment

The author wishes to thank Dr. E. M. T. Jones for his contributions and advice, and the members of the IBM Corporation Watson Scientific Computing Laboratory for their helpful suggestions and stimulating technical discussions during the course of this work.

Sets of Eigenvectors for Volumes of Revolution*

J. VAN BLADEL†

Summary—**The electric and magnetic eigenvectors of a volume of revolution can be written in terms of two-dimensional scalar and vector functions. These functions are the eigenfunctions of certain linear transformations in the meridian plane. The form of the transformation is examined, and much attention is devoted to the orthogonality properties of their eigenfunctions and the calculation of their eigenvalues from variational principles.**

AMONG the sets of eigenvectors which exist in a finite three-dimensional volume, the "electric" and "magnetic" modes are of particular importance for the calculation of electric and magnetic fields. The purpose of the present paper is to investigate the properties of these modes in volumes of revolution of the kind depicted in Fig. 1. An explicit mathematical expression can be given for the modes of a few simple volumes, such as the sphere and the coaxial cylinder, but in the most general case one has to resort to approximate procedures to obtain quantitative data. The most frequently used methods rely on the replacement of differential equations by difference equations, and on the use of variational principles for the calculation of eigenvalues. It is necessary, for a systematic application of these methods, to possess a precise classification and enumeration of the modes and their characteristics. This is what this paper, inspired by a previous analysis by Bernier,[1] sets out to provide.

The first structure to be examined will be the toroidal volume of Fig. 1(a), which is of importance for circular particle accelerators and, more generally, for ring-like structures through which particles or fluids are flowing. The fact that a toroidal volume does not contain any portion of the axis of revolution facilitates the mathematical formulation of the problem.

* Manuscript received by the PGMTT, September 22, 1959; revised manuscript received, October 11, 1959. Research supported by the Atomic Energy Commission, Contract No. AT(11-1)-384.

† Dept. of Electrical Engineering, University of Wisconsin, Madison, Wis.

[1] J. Bernier, "On electromagnetic resonators," *Onde élect.*, vol. 26, pp. 305–317; August–September, 1946.